Simulation and Visualization of Fluid Flows Around Real Objects in Augmented Reality

Xingze Tian and Tobias Günther

Department of Computer Science, ETH Zürich

Abstract

The long-term vision of augmented reality is to seamlessly integrate digital content into the real world, which provides new means to make physical processes visible that are usually invisible to the naked eye. One such example is the motion of air around us. With the help of a head-mounted augmented reality device, an interactive air flow simulation and the tracking of real-world objects, we develop a flow visualization tool box in which users interactively explore approximations of the real-world air flow around real objects. Since the flows respond dynamically to real-world objects, the influence of obstacle size and air flow speed on the creation and movement of vortices can be explored interactively using geometry-based flow visualization techniques, including pathlines and streaklines. We see our setup mainly used in an educational context or for science communication.

CCS Concepts

• ***Human-centered computing*** → ***Mixed / augmented reality; Scientific visualization;***

1. Introduction

Over the past decades, visionaries have repeatedly foreseen a future, in which augmented reality (AR) drastically changes our lives [LNO17]. AR is believed to have an enormous potential to revolutionize media consume, advertisement, and our instant access to information. Currently, head-mounted AR devices are heavy and relatively uncomfortable to wear over a longer period of time. The field of view, the spatial tracking and spatial understanding, as well as the processing power are limited these days. These problems, however, disappear in the near future, due to the continuous progress made in computer vision and engineering. With a new generation of AR hardware on the horizon, it is time to think more about the impact that augmented reality can have in visualization.

In traditional 2D visualization, spatial perception and 3D interaction are notoriously difficult. AR, on the other hand, allows for a direct 3D interaction, which can be beneficial in exploration tasks. Further, the augmentation of the real 3D world opens new possibilities. For instance, with AR it becomes imaginable to visualize real-world air flows, which are usually invisible to us. Especially for educational purposes and science communication, AR can become a tangible and engaging entry point.

In this paper, we develop an augmented reality setup that allows non-expert users to explore real-world air flows by geometry-based flow visualization. Our experimental setup consists of a fan (to provide haptic feedback of an incoming air flow), a head-mounted AR device to capture the real-world scene and to place 3D holograms, and a number of tangible objects [LNBK04] that are tracked and can be placed in an interactive GPU-based air flow simulation. In the AR environment, users can place real obstacles and particle seeding objects to explore vortex patterns, such as the development of a von-Kármán vortex street. Visualization parameters such as the type of integral curve and the inflow speed are controlled by the texture of the tangible objects or by voice command, respectively.

2. Related Work

Augmented Reality (AR) is a technology that embeds virtual information in the real world. In 1997, Azuma formally defined AR as real-time interactive system that is registered in 3D and merges virtual and real content [Azu97]. Computer vision techniques are commonly used to track and reconstruct the real environment for correct registration [CFA*11]. This enables accurate positioning of virtually added objects that can be viewed through head-mounted displays (HMD), hand-held devices or projected displays [ABB*01]. By now, a number of different professional applications have been explored, such as automotive, architecture and surgery assistance [KOGD*15].

Different visualization techniques have been developed for various AR applications and can be classified according to the data types as scalar fields, vector fields and tensor fields [SROG04]. The 3D data are typically visualized as 2D images and can be mixed with video stream or user's view for AR purposes with correct

DOI: 10.2312/evs.20191171

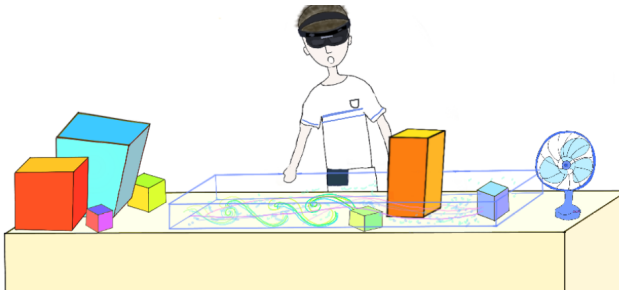

Figure 1: *Illustration of the hardware setup. Our system consists of a table workspace, a head-mounted display, tangible objects (obstacles and particle sources), and a fan for haptic feedback only.*

registration in 3D and time synchronization [SROG04]. Kersten-Oertel defined the DVV (Data, Visualization Processing, View) taxonomy for mixed reality visualization [KJC12] and used AR to assist neurovascular surgery by merging the live view of the patients and volume-rendered vessels [KOGD*15] using alpha blending, fogs and edges. Imahorn et al. [IBRG18] performed volume rendering of numerical simulation data of asteroid impacts on a head-mounted AR device. Collaborative AR has been developed to enable multiple users to study 3D data visualizations at the same time such as The CAVE [CNSD93] and STUDIERSTUBE [FLS97]. The latter uses a decoupled simulation approach [SGLS93] that separates the visualization system and the AR user interface that communicate each other via an AVS network [FLS97].

With the recent developments in hardware, AR technologies have emerged to accommodate mobile devices for visualizing scientific data that requires intensive computation. In the recent research, Kim et al. developed a system for reviewing computational fluid dynamics (CFD) in an AR content [KYJ*18]. The system performs simulation calculations in a cloud computing environment using the OpenFOAM solver, the results are then post-processed to reduce data volume and displayed on a handheld AR device [KYJ*18]. In contrast, we aim for a lighter setup that does not require cloud computing, but instead performs approximate calculations on the AR hardware itself.

3. AR Flow Toolbox

3.1. Goals and Scope

Our goal is to develop an augmented reality toolbox that allows non-expert users to interactively explore the motion of air flows around dynamic real-world objects. In particular, we concentrate on vortex dynamics [GT18] behind obstacles, such as the influence of obstacle size and inflow velocity on the creation of a von-Kármán vortex street. By using holograms, the 3D air flow is made visible and more tangible. Since we target non-expert users for educational purposes, we aim for a system that does not require extensive equipment, such as a camera-based tracking system or a cloud computing infrastructure. Instead, the object tracking, the approximate fluid simulation and the flow visualization are calculated directly on the user's head-mounted AR device.

3.2. System Overview

Hardware Setup. An overview of the hardware setup is shown in Fig. 1. The virtual simulation domain is placed as a hologram on the table workspace. The user wears a head-mounted AR display and can place tangible objects in the fluid simulation domain. Tangible objects include both obstacles and seeding objects, for which position and orientation are tracked by the AR device. For haptic feedback, a fan generates a slow air flow to increase the immersion.

Components. Our system contains the following components:

- a real-time fluid flow solver that reacts to the dynamic obstacles,
- a flow visualization that computes pathlines and streaklines,
- and a marker-based 3D tracking of tangible objects.

In the following sections, we explain the computational components in more detail. Afterwards, we describe the user interaction.

3.3. Fluid Simulation

Since we need a real-time fluid simulation that includes solid-fluid interactions, we use the real-time fluid flow solver of Crane et al. [CLT07]. Their GPU implementation is based on the stable fluid method of Stam [Sta99], which solves the Navier stokes momentum equation for incompressible and inviscid flows:

$$\frac{\partial \mathbf{u}}{\partial t} = -(\mathbf{u}\cdot\nabla)\mathbf{u} - \frac{1}{\rho}\nabla p + \mathbf{f}, \qquad \nabla\cdot\mathbf{v} = 0 \tag{1}$$

Following Harris [Har05], Crane et al. stored data on Eulerian (non-staggered) grids, used finite differences for derivative discretization and advected the flow with a two-step semi-Lagrangian scheme. Likewise, we used a MacCormack advection. Other choices are discussed by Crane et al. [CLT07]. As external force $\mathbf{f}$, a Bouyancy term is applied. The numerical solver alternates between advection and pressure projection to retain a divergence-free flow, and the dynamic obstacles are voxelized whenever they move. We refer to Crane et al. [CLT07] for implementation details. Note that the fluid simulation is only a rough approximation of the real-world fluid flow that is present in the experimental setup.

3.4. Flow Visualization

In order to make the simulated fluid flow $\mathbf{v}(\mathbf{x},t)$ visible, we employ basic geometry-based flow visualization methods [MLP*10].

Particles and Pathlines. To show particles and their trajectories, we compute tangent curves $\mathbf{p}(t)$, i.e., pathlines:

$$\frac{\mathrm{d}\,\mathbf{p}(t)}{\mathrm{d}t} = \mathbf{v}(\mathbf{p}(t),t), \qquad \mathbf{p}(t_0) = \mathbf{x}_0 \tag{2}$$

The seed point $(\mathbf{x}_0, t_0)$ is determined interactively by the user. We fade the transparency of pathlines from head to end to better convey the motion.

Streaklines. Advected flow patterns such as vortices are better shown by the use of streaklines [WWSS10, WT10], which connect particles that were continuously released from a common seed point. Using the flow map $\phi_{t_0}^{\tau}(\mathbf{x}_0)$, which returns the location that is

reached after duration τ by a particle seeded at $(\mathbf{x}_0, t_0)$, a streakline $\mathbf{s}(\tau, t)$ at the time of interest t is simply defined via:

$$\mathbf{s}(\tau, t) = \phi_{\tau}^{t-\tau}(\mathbf{x}_0) \tag{3}$$

Streaklines are computed by advection of a particle front, which usually requires refinement by subdivision when neighboring particles move too far apart. To avoid the subdivision (and dynamic allocation of geometry), we employ the smoke metaphor of von Funck et al. [VFWTS08], which keeps the line topology fixed and reduces the transparency if vertices drift apart.

3.5. Motion Tracking

The sensing system of our head-mounted augmented reality device leverages an inertial measurement unit (IMU) and a depth camera to track the motion of the device and to register its position in 3D. For correct registration, the device provides different real-world coordinate systems including stationary frame of reference, attached frame of reference, spatial anchor and spatial mapping. The first three are more suitable for small-scale applications and require the positioning of an object at a fixed position or a user-placed anchor. The spatial mapping directly scans and maps the real environment as virtual surfaces and is more suitable for large-scale applications. For the scale of our experimental setup, we use a stationary frame of reference by default that our simulation domain is placed at. We also provide the capability of selecting a world anchor and place the whole simulation domain by the tapping gesture.

In addition to the intrinsic tracking abilities of the augmented reality device, we use a marker-based tracking library to track the seeding sources and obstacles. The tracking system analyses the RGB camera stream and detects real images or objects that have previously been uploaded to a database. The tracking system returns the extracted 3D position and pose of the tracked seeds boxes and obstacles, and we update our visualization accordingly, when users interact with the tracked objects.

3.6. User Interaction

The simulation domain is either placed at a fixed pre-determined location or by placing a hologram on a table or surface to choose the reference point. Users can move different seed boxes to determine the seed positions and and texture of the boxes determines the visualization method (pathlines and streaklines). Further, users may place one or more obstacles in the simulation domain to explore fluid dynamical processes. The maximum number of objects is limited by Vuforia. Due to the domain size, we never used more than three obstacles and two seed boxes. Finally, users can change the inflow velocity via voice commands by saying "faster" or "slower" and can also enable or disable one or more visualization methods by voice commands, such as the particle rendering.

4. Implementation

Setup. As head-mounted augmented reality device, we use Microsoft HoloLens [Hol]. For development, we use Visual Studio 2017 [Vis] and Unity 2017.4.1f [Uni] with Vuforia [Vuf] and the Microsoft Mixed Reality Toolkit (MRTK) [MRT]. The above Unity version integrates the texture-based tracking library Vuforia, from which we use image targets and cuboid targets for tracking. To enable the AR experience, a Unity build is generated and deployed on the device. This way, simulation, tracking and visualization are all performed on the device. The voice commands are implemented using the Microsoft Mixed Reality Toolkit, which recognizes a set of given target words or phrases.

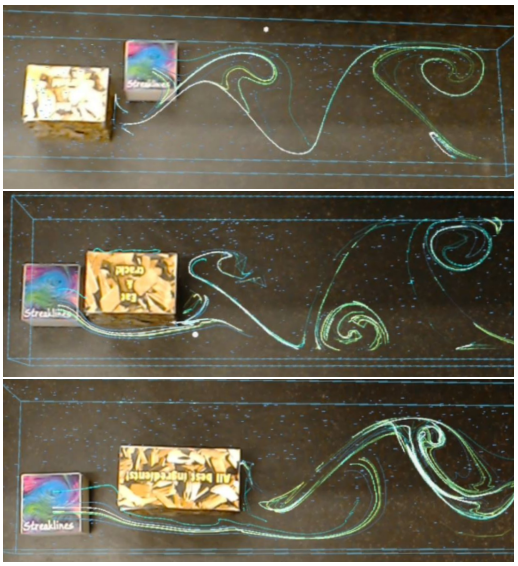

Figure 2: *Screen captures taken for varying obstacle positions, orientations and seeding box positions.*

Visualization. The advection of particles, pathlines and streaklines is performed with compute shaders. Each particle is initialized at a relative position in the seeding box and is advected each frame with the fluid flow. Once a particle is expired or left the domain, it is reseeded at the same initial position. Since Unity does not support transform feedback, i.e., the adaptive generation of geometry in a geometry shader, we keep a fixed line topology for the streaklines and apply the transparency mapping of von Funck et al. [VFWTS08] to resemble smoke lines. We implemented different shaders for rendering various components of the system. Particles are rendered as splats and pathlines and streaklines are rendered as viewport-aligned triangle strips. We used a different color palette for pathlines and streaklines and gave each line a different color. It would be imaginable to color-code fluid flow attributes.

To seamlessly integrate the augmented objects into the real scene, we render proxies of the real-world obstacles at the tracked position into the depth buffer. Thus, augmented objects such as particles and streaklines can be clipped when they are occluded by a real obstacle. We chose to disable this feature for the seeding objects, since particles and streaklines are seeded inside the box.

5. Results

5.1. Interactive Sessions

Next, we show screen captures from the users view. We refer to the accompanying video for recordings of interactive sessions.

Figure 3: *Visualizations of the flow patterns created when using different obstacle sizes. Top: small obstacle, bottom: large obstacle.*

Grid resolution	Frame rate
$64 \times 8 \times 16$	36 *fps*
$128 \times 8 \times 32$	35 *fps*
$256 \times 16 \times 64$	27 *fps*

Table 1: *Frame rate measurements for varying simulation grids.*

Obstacle and Seeding Position. In Fig. 2, we show varying fluid flows that arise for different obstacle placements and orientations. The user also placed the streakline seeding box at different locations to show the flow around the obstacle, as well as the path of particles seeded behind the obstacle.

Obstacle Sizes. Fig. 3 shows that bigger obstacles have a larger recirculation area in the wake of the obstacle. Therefore, the velocity magnitude is lower in a larger area, leading to a more prominent formation of a vortex street.

Inflow Velocity. In Fig. 4, we show streak-line based visualizations for varying inflow velocities. In contrast to the fast case, the slower case forms vortices downstream. Both settings exhibit a recirculation bubble directly in the wake of the obstacle.

5.2. Performance

The choice of the simulation grid resolution is a trade-off between performance and detail. We experimented with different resolutions and report the timings in Table 5.2. If the resolution is too low, small-scale flow patterns cannot be resolved. On the other hand, if the resolution is very high, the frame rate decreases too much. We empirically chose a simulation grid resolution of $128 \times 32 \times 8$ voxels, for which we achieved a constant frame rate of 35 frame per second. Note that we measured the performance of the entire setup at full workload using Windows device portal, i.e., including numerical flow simulation, particle advection, streakline advection, object tracking and voice recognition.

6. Discussion

Approximation. The fluid flow simulation is a very coarse approximation to the real-world flow, since we use a computer graphics method [CLT07]. Thus, the tool box can only have an educational character, demonstrating fluid flow patterns. In the future, we would like to improve the matching between real-world and approximate simulation, i.e., use more controlled lab conditions in the experimental setup (such as boundary conditions) and a fluid simulation with experimentally validated accuracy. For the didactic purpose, the simplified setup was sufficient, since the vortex street appeared as expected.

Figure 4: *Flow visualizations, showing the impact of different inflow velocities on the vortex patterns. Top: slow inflow velocity, bottom: fast inflow velocity.*

Scalability. At present, both simulation and rendering are carried out on the AR device. In order to allow for larger simulation domains, it is imaginable to run the simulation on a server and to stream the rendered images for final display, similar to the approach discussed by Kim et al. [KYJ*18]. The main limitation is the streaming bandwidth and the potential delay. For non-expert users, we preferred a light-weight setup.

7. Conclusion

In this paper, we described an augmented reality framework, in which non-expert users can explore numerically-simulated air flows around real-world obstacles that can be moved interactively. By running the numerical fluid simulation, the motion tracking and the geometry-based flow visualization on the head-mounted augmented reality device, we enable users to study the impact of inflow velocity and obstacle size on the creation of vortices.

For the future, we consider to move some of the calculations to a remote desktop in order to increase performance. We think that augmented reality will be valuable for science communication, when used by non-expert users. The perception of color, however, is strongly affected by the background and the illumination conditions, making the precise reading of color information near impossible. For this reason, we think that color coding in augmented reality settings is currently not feasible for scientific data analysis. Finally, we would like to explore non-photorealistic rendering techniques to make the visualization more accessible.

Acknowledgments

This work was partially funded by the ETH Zurich Career Seed Grant SEED-06 17-2.

References

[ABB*01] AZUMA R., BAILLOT Y., BEHRINGER R., FEINER S., JULIER S., MACINTYRE B.: Recent advances in augmented reality. *IEEE Computer Graphics and Applications 21*, 6 (Nov 2001), 34–47. 1

[Azu97] AZUMA R. T.: A survey of augmented reality. *Presence: Teleoperators and Virtual Environments 6*, 4 (1997), 355–385. 1

[CFA*11] CARMIGNIANI J., FURHT B., ANISETTI M., CERAVOLO P., DAMIANI E., IVKOVIC M.: Augmented reality technologies, systems and applications. *Multimedia Tools and Applications 51*, 1 (Jan 2011), 341–377. 1

[CLT07] CRANE K., LLAMAS I., TARIQ S.: Real-time simulation and rendering of 3D fluids. *GPU Gems 3*, 1 (2007), 633–675. 2, 4

[CNSD93] CRUZ-NEIRA C., SANDIN D. J., DEFANTI T. A.: Surround-screen projection-based virtual reality: the design and implementation of the CAVE. In *SIGGRAPH '93: Proceedings of the 20th annual conference on Computer graphics and interactive techniques* (New York, NY, USA, 1993), ACM, pp. 135–142. 2

[FLS97] FUHRMANN A., LOFFELMANN H., SCHMALSTIEG D.: Collaborative augmented reality: exploring dynamical systems. In *Proceedings. Visualization '97 (Cat. No. 97CB36155)* (Oct 1997), pp. 459–462. 2

[GT18] GÜNTHER T., THEISEL H.: The state of the art in vortex extraction. *Computer Graphics Forum 37*, 6 (2018), 149–173. 2

[Har05] HARRIS M. J.: Fast fluid dynamics simulation on the GPU. *SIGGRAPH Courses 220* (2005). 2

[Hol] Microsoft HoloLens. http://hololens.com/. Accessed: 2019-04-02. 3

[IBRG18] IMAHORN R., BAEZA ROJO I., GÜNTHER T.: Visualization and analysis of deep water asteroid impacts. In *IEEE Scientific Visualization Contest* (2018). 2

[KJC12] KERSTEN-OERTEL M., JANNIN P., COLLINS D. L.: DVV: A taxonomy for mixed reality visualization in image guided surgery. *IEEE Transactions on Visualization and Computer Graphics 18*, 2 (Feb 2012), 332–352. 2

[KOGD*15] KERSTEN-OERTEL M., GERARD I., DROUIN S., MOK K., SIRHAN D., SINCLAIR D. S., COLLINS D. L.: Augmented reality in neurovascular surgery: feasibility and first uses in the operating room. *International journal of computer assisted radiology and surgery 10*, 11 (2015), 1823–1836. 1, 2

[KYJ*18] KIM M., YI S., JUNG D., PARK S., SEO D.: Augmented-reality visualization of aerodynamics simulation in sustainable cloud computing. *Sustainability (2071-1050) 10*, 5 (2018). 2, 4

[LNBK04] LEE G. A., NELLES C., BILLINGHURST M., KIM G. J.: Immersive authoring of tangible augmented reality applications. In *Proceedings of the 3rd IEEE/ACM international Symposium on Mixed and Augmented Reality* (2004), IEEE Computer Society, pp. 172–181. 1

[LNO17] LI W., NEE A., ONG S.: A state-of-the-art review of augmented reality in engineering analysis and simulation. *Multimodal Technologies and Interaction 1*, 3 (2017), 17. 1

[MLP*10] MCLOUGHLIN T., LARAMEE R. S., PEIKERT R., POST F. H., CHEN M.: Over two decades of integration-based, geometric flow visualization. *Computer Graphics Forum 29*, 6 (2010), 1807–1829. 2

[MRT] Microsoft mixer reality toolkit. https://microsoft.github.io/MixedRealityToolkit-Unity. Accessed: 2019-04-02. 3

[SGLS93] SHAW C. D., GREEN M., LIANG J., SUN Y.: Decoupled simulation in virtual reality with the MR toolkit. *ACM Trans. Inf. Syst. 11*, 3 (1993), 287–317. 2

[SROG04] SILVA R. L., RODRIGUES P. S., OLIVEIRA J. C., GIRALDI G.: Augmented reality for scientific visualization: Bringing data sets inside the real world. *LNCC–National Laboratory for Scientific Computing, Petropolis, RJ, Brazil* (2004). 1, 2

[Sta99] STAM J.: Stable fluids. In *Siggraph* (1999), vol. 99, pp. 121–128. 2

[Uni] Unity. https://unity.com/. Accessed: 2019-04-02. 3

[VFWTS08] VON FUNCK W., WEINKAUF T., THEISEL H., SEIDEL H.-P.: Smoke surfaces: An interactive flow visualization technique inspired by real-world flow experiments. *IEEE Transactions on Visualization and Computer Graphics 14*, 6 (2008), 1396–1403. 3

[Vis] Microsoft visual studio. https://visualstudio.microsoft.com. Accessed: 2019-04-02. 3

[Vuf] Vuforia. https://www.vuforia.com/. Accessed: 2019-04-02. 3

[WT10] WEINKAUF T., THEISEL H.: Streak lines as tangent curves of a derived vector field. *IEEE Transactions on Visualization and Computer Graphics 16*, 6 (Nov 2010), 1225–1234. 2

[WWSS10] WIEBEL A., WANG Q., SCHNEIDER D., SCHEUERMANN G.: Accelerated streak line computation using adaptive refinement. *Journal of WSCG 18* (2010), 17–23. 2